

# FAST CALIBRATION TECHNIQUE FOR A GIMBALLED INERTIAL NAVIGATION SYSTEM

**Yong-Jin Shin, Jeong-Hwa Park**  
**Agency for Defense Development, Yuseong P.O.Box 35-5**  
**305 600 Daejeon, Korea**

**Cheon-Joong Kim**  
**Korea Aerospace Research Institute, Yuseong P.O.Box 113**  
**305 600 Daejeon, Korea**

**Keywords:** *calibration, gimbaled INS, Kalman filtering, Schuler factor*

## Abstract

*The performance of inertial navigation system (INS) is largely dependent on calibration errors of gyroscopes and accelerometers. A typical gimbaled INS is calibrated while stationary by multi-position rotating the inertial platform relative to the earth's spin axis and local gravity vector in order to excite the gyroscope and accelerometer parameters. And, there is another technique which inertial sensor parameters are estimated by least square method using velocity errors obtained from so-called single-axis Schuler calibration test in navigation mode. These have led to lengthy calibration procedures.*

*In this study, we propose the fast calibration technique by Kalman filtering with the modified level axis Schuler error loop in which the Schuler factor is introduced in order to be able to change the Schuler period. The simulation results show that the calibration accuracy is improved as the Schuler period is decreased. Furthermore, fast calibration results from reducing the Schuler period.*

*Consequently, our proposed calibration technique has led to enhanced accuracy in the instrument errors estimation while reducing the calibration test time.*

## 1 Introduction

The performance of inertial navigation system (INS) is largely affected by the accuracy of inertial sensors. The velocity errors of INS

depend on calibration errors of gyroscopes and accelerometers, as well as attitude errors. Accurate calibration of inertial sensors is increasingly important as INS requirements become more stringent. Various calibration techniques for gimbaled or strapdown INS have been developed that accelerometer errors and gyroscope errors can be estimated by multi-position testing [1,2,3]. Most of the methods are similar in nature that they excite instrument errors through gimbals or system rotations.

This paper focuses upon a gimbaled INS with floated rate integrating gyroscopes and pendulous accelerometers. A typical gimbaled INS, in calibration alignment mode, is calibrated while stationary by multi-position rotating the inertial platform relative to the earth's spin axis and local gravity vector in order to excite the gyroscope and accelerometer parameters. And, there is another technique which inertial sensor parameters are estimated by least square method using velocity errors obtained from so-called single-axis Schuler calibration test in navigation mode. If large initial velocity error in a horizontal channel of a gimbaled INS is given while stationary, gimbals attitude is oscillatory changed. It is a basic principle of the single-axis Schuler calibration test. These have led to lengthy calibration procedures. It takes about 5 hours or more for completion of the calibration procedures.

The application of Kalman filtering to the calibration of a gimbaled INS has been reported

in numerous papers [4,5,6]. For estimating instruments errors accurately, the measurement process should be rapid in order to reduce sensitivity to noise and random drifts.

In this paper, we propose the fast calibration technique by Kalman filtering with the modified level axis Schuler error loop in which the Schuler factor is newly introduced in order to be able to change the Schuler period intentionally. The quaternion attitude error equation is augmented by gyroscope errors and accelerometer errors, and a linear Kalman filter as calibration filter is developed to estimate the instrument parameters.

## 2 INS Error Characteristics

The error characteristic of an INS for the computation of velocity and attitude is described by the sinusoidal Schuler oscillation that has a period of approximately 84.4 minutes. The schematic block diagram of the modified level axis Schuler error loop, in which newly introduced Schuler factor  $K_{SF}$  is included, is illustrated in Fig. 1.

First, for the familiar level axis Schuler error loop when  $K_{SF}$  equals 1, velocity and attitude error equations are reviewed. Let  $\delta v(0)$  be initial velocity error input,  $\varepsilon(0)$  be assumed initial attitude error,  $\delta w(t)$  and  $\delta f(t)$  be gyroscope error and accelerometer error respectively. Then the velocity error equation is described as equation (1).

$$\delta V(s) = \frac{1}{\Delta(s)} [s \delta f(s) + g \delta w(s) + s \delta v(0) - g \varepsilon(0)] \quad (1)$$

where  $\Delta(s)$  is the characteristic equation as

$$\Delta(s) = s^2 + \omega_s^2 \quad (2)$$

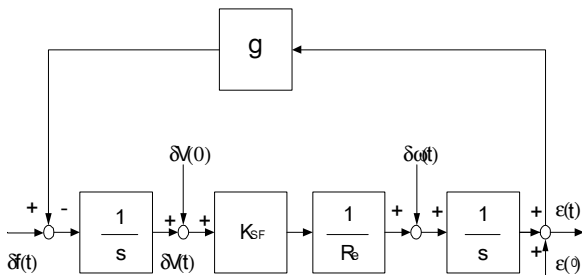


Fig. 1. Modified Level axis Schuler error loop ( $K_{SF}$  equals 1 for familiar Schuler error loop).

In above equation (2),  $\omega_s$  denotes the Schuler frequency corresponding to the Schuler period  $T_s$ , which is defined by the expression

$$T_s = \frac{2\pi}{\omega_s} = 2\pi \sqrt{\frac{R_e}{g}} \approx 84.4 \text{ min} \quad (3)$$

where  $R_e$  is the earth radius. Taking the inverse Laplace transform of equation (1), velocity error equation is written as following:

$$\begin{aligned} \delta v(t) = & \frac{\delta f(t)}{\omega_s} \sin \omega_s t + \frac{\delta w(t)g}{\omega_s^2} (1 - \cos \omega_s t) \\ & + \delta v(0) \cos \omega_s t - \frac{g}{\omega_s} \varepsilon(0) \sin \omega_s t \end{aligned} \quad (4)$$

Note that the maximum velocity error appeared due to the given initial velocity error input is not dependent upon the Schuler frequency, while the effect caused by accelerometer error or initial attitude error is inversely proportional to the Schuler frequency and the effect caused by gyroscope error is inversely proportional to the square of the Schuler frequency.

Likewise, attitude error equation can be derived as equation (5).

$$\begin{aligned} \varepsilon(t) = & \frac{\delta f(t)}{R_e \omega_s^2} (1 - \cos \omega_s t) + \frac{\delta w(t)}{\omega_s} \sin \omega_s t \\ & + \varepsilon(0) \cos \omega_s t + \frac{\delta v(0)}{R_e \omega_s} \sin \omega_s t \end{aligned} \quad (5)$$

Note that maximum attitude error induced due to the given initial velocity error input or gyroscope error is inversely proportional to the Schuler frequency and the effect caused by accelerometer error is inversely proportional to the square of the Schuler frequency, while the effect caused by initial attitude error is not dependent upon the Schuler frequency.

Now, for the modified level axis Schuler error loop, velocity and attitude error equations including the Schuler factor  $K_{SF}$  are discussed. The modified characteristic equation and the modified Schuler period can be stated as followings:

$$\Delta_{SF} = s^2 + \omega_{SF}^2 \quad (6)$$

$$T_{SF} = \frac{2\pi}{\omega_{SF}} = 2\pi \sqrt{\frac{R_e}{K_{SF} g}} \quad (7)$$

Hereby, velocity and attitude error equations including the Schuler factor  $K_{SF}$  are derived as followings:

$$\begin{aligned} \delta v(t) &= \frac{\delta f(t)}{\omega_{SF}} \sin \omega_{SF} t + \frac{\delta w(t)g}{\omega_{SF}^2} (1 - \cos \omega_{SF} t) \\ &\quad + \delta V(0) \cos \omega_{SF} t - \frac{g}{\omega_{SF}} \varepsilon(0) \sin \omega_{SF} t \end{aligned} \quad (8)$$

$$\begin{aligned} &= \frac{\delta f(t)}{\sqrt{K_{SF} \omega_s}} \sin \omega_{SF} t + \frac{\delta w(t)g}{K_{SF} \omega_s^2} (1 - \cos \omega_{SF} t) \\ &\quad + \delta v(0) \cos \omega_{SF} t - \frac{g}{\sqrt{K_{SF} \omega_s}} \varepsilon(0) \sin \omega_{SF} t \\ \varepsilon(t) &= \frac{\delta f(t)K_{SF}}{R_e \omega_{SF}^2} (1 - \cos \omega_{SF} t) + \frac{\delta w(t)}{\omega_{SF}} \sin \omega_{SF} t \\ &\quad + \varepsilon(0) \cos \omega_{SF} t + \frac{K_{SF}}{R_e \omega_{SF}} \delta v(0) \sin \omega_{SF} t \\ &= \frac{\delta f(t)}{R_e \omega_s^2} (1 - \cos \omega_{SF} t) + \frac{\delta w(t)}{\sqrt{K_{SF} \omega_s}} \sin \omega_{SF} t \\ &\quad + \varepsilon(0) \cos \omega_{SF} t + \sqrt{\frac{K_{SF}}{g R_e}} \delta v(0) \sin \omega_{SF} t \end{aligned} \quad (9)$$

Above equation (8) shows that the maximum velocity error appeared due to the given initial velocity error input is not dependent upon the Schuler factor  $K_{SF}$ , while the effect caused by accelerometer error or initial attitude error is inversely proportional to the square root of the Schuler factor  $K_{SF}$  and the effect caused by gyroscope error is inversely proportional to the Schuler factor  $K_{SF}$ . And, equation (9) shows that the maximum attitude error induced due to the given initial velocity error input is proportional to the square root of the Schuler factor  $K_{SF}$ , while the effect caused by gyroscope error is inversely proportional to the square root of the Schuler factor  $K_{SF}$ .

### 3 Formulation of a Calibration Filter

A linear Kalman filter is developed for the calibration of a gimbaled inertial navigation system. This technique uses the navigation outputs of a gimbaled INS. These outputs,

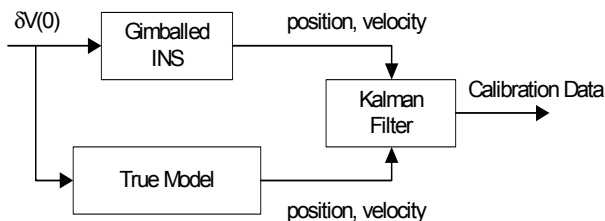


Fig. 2. Block diagram of INS calibration.

velocity and position obtained by calculating the navigation equation assuming that initial velocity error  $\delta v(0)$  only exists, are processed by the Kalman filter. A simplified schematic block diagram is shown in Fig. 2. Total state vector of Kalman filter include system errors such as attitude error, horizontal velocity and position error states and sensor errors such as gyroscope and accelerometer error states.

As mentioned earlier, gimbals attitude is oscillatory changed if large initial velocity error in a horizontal channel is given in a gimbaled INS while stationary. Therefore, velocity and position error are generated by the given initial velocity error. Position and velocity in the true model in which does not include any sensor errors are calculated by navigation algorithm at error free  $p'$  coordinate frame. They are used as reference measurements in calculating the system matrix of Kalman filter. While, position and velocity in the erroneous gimbaled INS model are calculated by navigation algorithm at error-corrupted  $p$  coordinate frame. The difference between the outputs of the true model and the outputs of the erroneous gimbaled INS model are used as measurement inputs of Kalman filter.

Velocity and attitude differential equations at  $p'$  and  $p$  frame can be written as equations (10)-(13).

$$\dot{V}^{p'} = C_n^{p'} f^n + (2w_{ie}^{p'} + w_{ep}^{p'}) \times V^{p'} + g^{p'} \quad (10)$$

$$\begin{aligned} \dot{C}_p^n &= C_p^n \Omega_{np}^{p'} \\ &= C_p^n \Omega_{ip}^{p'} - \Omega_{in}^n(0) C_p^n \end{aligned} \quad (11)$$

$$\dot{V}^p = C_n^p f^n + (2w_{ie}^p + w_{en}^p) \times V^p + g^p \quad (12)$$

$$\begin{aligned} \dot{C}_p^n &= C_p^n \Omega_{np}^p \\ &= C_p^n \Omega_{ip}^p - \Omega_{in}^n(0) C_p^n \end{aligned} \quad (13)$$

In the above equations,  $\Omega_{in}^n(0)$  is the earth rate at test position. Acceleration and angular rate at  $p$  frame are modeled as followings:

$$f^p = f^{p'} + \delta f^p \quad (14)$$

$$w_{ip}^p = w_{ip}^{p'} + \delta w_{ip}^p \quad (15)$$

where  $\delta f^p$  is accelerometer error and  $\delta w_{ip}^p$  is gyroscope error.

Using the navigation equations at two frames, velocity and attitude error differential

equations of a gimbaled INS can be derived as equation (16) and (17). In this paper, quaternion attitude error equation is derived for the attitude error computation, because the quaternion attitude error equation is more effective than the Euler angle error equation in the case of larger attitude error.

$$\delta \dot{V}^{p'} = -2f^{p'} \times S(q)^T + (2\delta w_{ie}^{p'} + \delta w_{ep}^{p'}) \times V^{p'} + (2w_{ie}^{p'} + w_{ep}^{p'}) \times \delta V^{p'} + \delta f^{p'} + \delta g \quad (16)$$

$$\delta \dot{Q} = \frac{1}{2} [w_{ip}^{p'}]_A \delta Q - \frac{1}{2} [w_{in}^n(0)]_B \delta Q - \frac{1}{2} T(q) \delta w_{ip}^{p'} \quad (17)$$

where

$$T(q) = \begin{bmatrix} -q_1 & -q_2 & -q_3 \\ q_0 & -q_3 & q_2 \\ q_3 & q_0 & -q_1 \\ -q_2 & q_1 & q_0 \end{bmatrix} \quad (18)$$

$$S(q) = \begin{bmatrix} -q_1 & -q_2 & -q_3 \\ q_0 & q_3 & -q_2 \\ -q_3 & q_0 & q_1 \\ q_2 & -q_1 & q_0 \end{bmatrix} \quad (19)$$

Note that  $[w_{in}^n(0)]_B$  and the sign of  $T(q)\delta w_{ip}^{p'}$  in the above quaternion attitude error equation for the proposed calibration of a gimbaled INS are different from those in the known quaternion attitude error equation used in a strapdown INS.

Using the above equations, state and measurement equations of the calibration filter are described as

$$\dot{x}(t) = Fx(t) + Gw(t) \quad (20)$$

$$z(t) = Hx(t) + v(t) \quad (21)$$

Total state vector of Kalman filter include system errors such as attitude error, horizontal velocity and position error states and sensor errors such as gyroscope and accelerometer error states. The dimension of Kalman filter is 19<sup>th</sup> order. The system error state vector consists of two horizontal position errors, two horizontal velocity errors, and four quaternion attitude error states. Vertical position and velocity errors are excluded in order to prevent the divergence of Kalman filter estimation. The sensor error state vector consists of three gyroscope bias errors, four level gyroscope g-sensitive errors, two level accelerometer bias errors, and two level accelerometer scale factor error states.  $F$  matrix in equation (20) is a system matrix

including system error and sensor error model, and  $w(t)$  is white process noise which has zero mean and covariance of  $Q$ . The difference between the reference position, velocity output from the true model and the position, velocity output from the erroneous gimbaled INS model is used as a measurement vector of Kalman filter. In equation (21),  $v(t)$  is white gaussian measurement noise, which has zero mean and covariance of  $R$ . Detailed derivation of matrix  $F$  and  $H$  in equation (20), (21) is omitted in this paper, refer to [6,8,9].

## 4 Simulation Results and Discussion

In order to simulate the effect on the calibration filter performance and error propagation characteristics related to the change in the Schuler period,  $K_{SF}$  is varied from 1/16, 1/4, 1, 4, to 16. We assumed accelerometer bias error is 100 micro-g, scale factor error is 300 ppm, gyroscope g-sensitive error is 0.2 deg/hr/g, and bias errors of level gyroscope and vertical gyroscope are 0.01 deg/hr and 0.1 deg/hr, respectively. These are 1-sigma values.

### 4.1 Error Propagation Characteristics

First, the velocity and attitude error propagation characteristics related to the change in the Schuler period is reviewed. While the Schuler factor  $K_{SF}$  is changed from 1/16, 1/4, 1, 4, to 16, an initial east velocity error input  $\delta v(0)$  is set to 1,500ft/sec. East velocity error propagation characteristic in the  $p'$  frame is shown in Fig. 3. It is shown that the change in the Schuler factor  $K_{SF}$  has an effect on the Schuler period only, but not on the maximum velocity error as stated in equation (8). To check the velocity error propagation characteristics due to inertial sensor error, we made an assumption that east accelerometer bias only exists. East velocity error propagation characteristic in the  $p'$  frame is shown in Fig. 4. As stated in equation (8), the maximum velocity error caused by accelerometer error is inversely proportional to the square root of the Schuler factor  $K_{SF}$ . And, the effect caused by gyroscope error is inversely

proportional to the Schuler factor  $K_{SF}$  as shown in equation (8).

Now, in order to check the attitude error propagation characteristics related to the change in the Schuler period, an initial east velocity error input  $\delta v(0)$  is set to 1,500ft/sec while the Schuler factor  $K_{SF}$  is changed from 1/16, 1/4, 1, 4, to 16. The north axis attitude error propagation characteristic is shown in Fig. 5. It is shown that the maximum attitude error induced due to given initial velocity error input  $\delta v(0)$  is proportional to the square root of the Schuler factor  $K_{SF}$  as stated in equation (9). In addition, the larger  $K_{SF}$  is, the more angular movement of the gimbal becomes. Thus the effect of the gyroscope g-sensitive error is probably more increased. With an initial velocity error of 1,500ft/sec, the acceleration

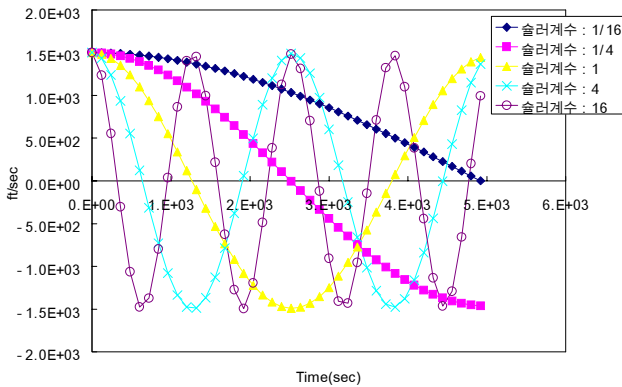


Fig. 3. Velocity error characteristics caused by given initial velocity error input.

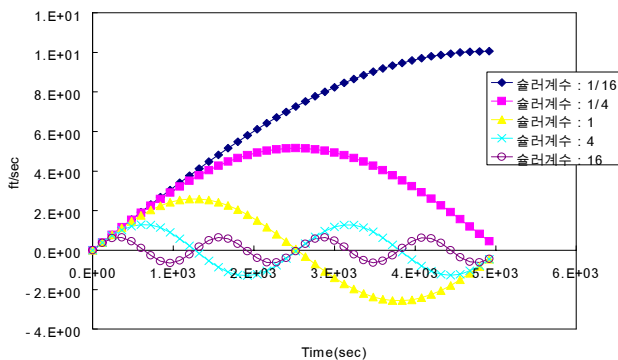


Fig. 4. Velocity error characteristics caused by accelerometer bias.

propagation characteristics in the  $p'$  frame is shown in Fig. 6. As shown in Fig. 5 and 6, the attitude error and resulting acceleration due to the given initial velocity error input  $\delta v(0)$  increase proportionally to the square root of the Schuler factor  $K_{SF}$ . It is believed that the detectability of the gyroscope g-sensitive error is improved as  $K_{SF}$  is increased.

#### 4.2 Performance of Calibration Filter

With varying the Schuler factor  $K_{SF}$ , the performance of the calibration filter was simulated by using the Monte-Carlo simulation technique. For the initial covariance of sensor error state variables, earlier mentioned 1-sigma values of sensor parameters were used. Simulations are performed assuming that the alignment of gimbaled INS has been completed

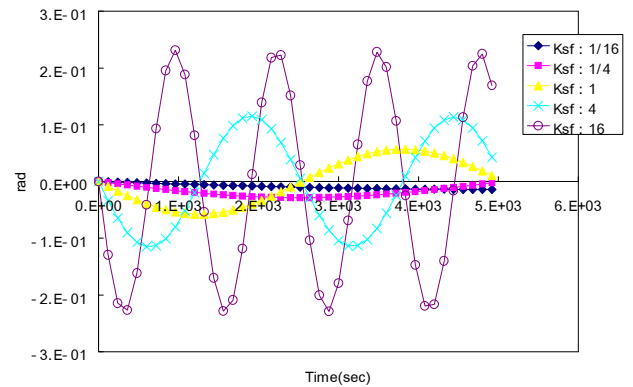


Fig. 5. Attitude error characteristics caused by given initial velocity error input.

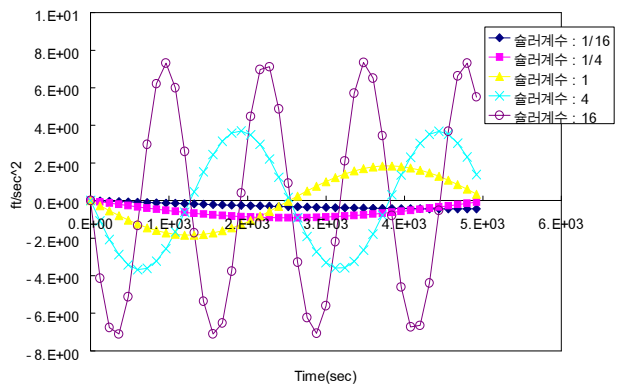


Fig. 6. Acceleration by attitude change.



and that initial east velocity of 1,500 ft/sec has been applied immediately after switching to navigation mode. Initial alignment error and the sensor errors are included in the simulation conditions.

The simulation results show that the estimation performance of a filter is improved proportionally to the value of the Schuler factor, and the best estimation performance of the Kalman filter is found when the Schuler factor is set to 16. It is believed that as the Schuler factor increases the estimation performance of the Kalman filter is improved because of the increased detectability resulting from greater attitude and acceleration. Fig. 7, 8 and 9 represent the simulation results of the estimation performance for the north gyroscope bias error, north gyro g-sensitive error, and east accelerometer bias error, respectively. As shown in Fig. 7 and 9, the estimation error convergence characteristics and Kalman filter estimation performance regarding the gyroscope bias and accelerometer bias are improved proportionally to the Schuler factor  $K_{SF}$ . There is more significant improvement in estimating the accelerometer bias error. Estimating the accelerometer bias is difficult in the beginning of the calibration process because of initial alignment error, but it is increasingly converged since angular tilt is larger as time goes. As shown in Fig. 8, estimating the gyroscope g-sensitive error is very difficult since the maximum attitude change is below 3 degree when the Schuler factor was less than 1. However, when the Schuler factor was set to a larger value, which also means a shorter Schuler period, the angular movement of the gimbal increased. This results in a significant improvement in gyroscope g-sensitive error estimation performance and convergent speed. Similar results were obtained for the estimation performance of other errors.

According to the above simulation results, when the Schuler factor is chosen to the adequate value more than 4, considerable improvement can be made in reducing the calibration time as well as filter performance. Although a larger Schuler factor  $K_{SF}$  results in

higher filter estimation performance, almost no improvement can be found for value larger than

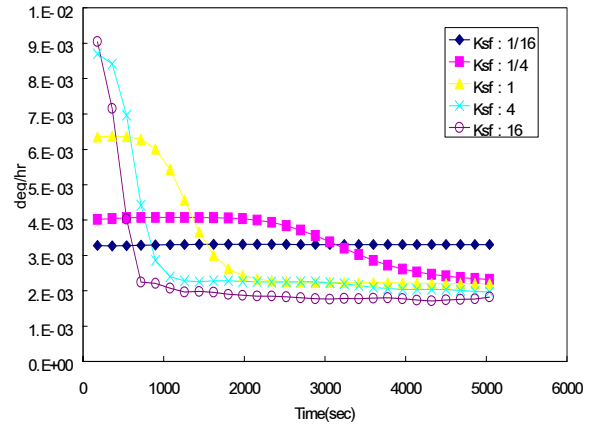


Fig. 7. Estimation performance for gyroscope bias error.

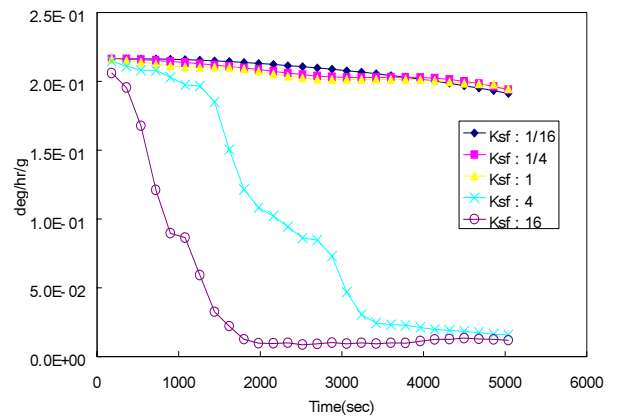


Fig. 8. Estimation performance for gyroscope g-sensitive error.

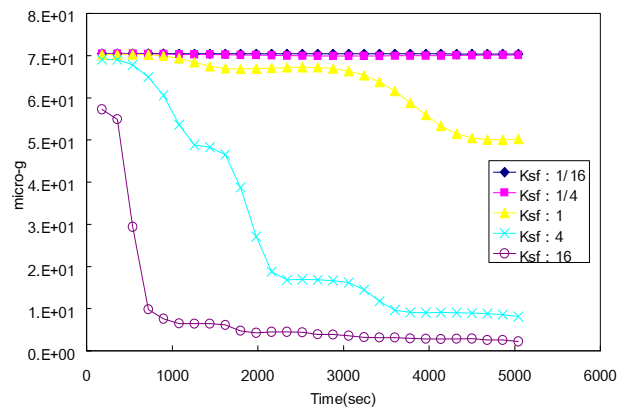


Fig. 9. Estimation performance for accelerometer bias error.

16. This is because the attitude change, which is the gimbal angular motion, becomes larger than 12 degree and enters a non-linear region when the Schuler factor  $K_{SF}$  is set to a value larger than 16.

Summarizing the simulation results, the calibration accuracy is improved as Schuler factor is increased or Schuler period is decreased. In particular, g-sensitive error estimation performance is significantly enhanced as the Schuler factor is 4 or more. Moreover, fast calibration results from reducing the Schuler period.

## 5 Conclusion

We discussed the fast calibration technique by Kalman filtering with the modified level axis Schuler error loop in which the Schuler factor is introduced in order to be able to change the Schuler period intentionally. The quaternion attitude error equation was augmented by gyroscope and accelerometer parameters, and a linear Kalman filter was developed to estimate the instrument parameters.

For the modified level axis Schuler error loop, velocity and attitude error equations including the Schuler factor were derived. The maximum velocity error appeared due to the given initial velocity error input is not dependent upon the Schuler factor, while the effect caused by accelerometer error or initial attitude error is inversely proportional to the square root of the Schuler factor and the effect caused by gyroscope error is inversely proportional to the Schuler factor. And, The maximum attitude error induced due to the given initial velocity error input is proportional to the square root of the Schuler factor, while the effect caused by gyroscope error is inversely proportional to the square root of the Schuler factor.

The simulation results show that the calibration accuracy is improved as the Schuler factor is increased or the Schuler period is decreased. In particular, gyroscope g-sensitive error estimation performance is significantly enhanced as the Schuler factor is increased. Moreover, fast calibration results from reducing

the Schuler period. Consequently, our proposed calibration technique has led to enhanced accuracy in the instrument errors estimation while reducing the calibration time.

## References

- [1] Krogmann U. Identification procedures for strapdown sensor parameter by laboratory testing. *DGON symposium gyro technology*, Germany, 1978.
- [2] Camberlein L and Mazzanti F. Calibration technique for laser gyro strapdown inertial navigation systems. *DGON symposium gyro technology*, Germany, 1985.
- [3] *Software design document for inertial navigation system*. GEC-Ferranti Ltd., 1990.
- [4] Grewal M. S, Henderson V. D and Miyasako R. S. Application of Kalman filtering to the calibration and alignment of inertial navigation systems. *IEEE Transactions on Automatic Control*, Vol. 36, No. 1, pp 4-13, 1991.
- [5] Kim K. J and Song T. L. Calibration of gimbaled inertial navigation systems using state estimation. *Journal of Control, Automation and Systems Engineering*, Vol. 4, No. 1, pp 62-67, 1998.
- [6] Park J. H, Kim C. J, Park H. W and Shin Y. J. An implementation of INS calibration technique using the velocity initialization. *Proceedings of the 12<sup>th</sup> KACC*, Korea, 1997.
- [7] Choi S. W, Kim C. J, Lee Y. S and Park H. W. Error propagation characteristics of inertial navigation system according to the change of Schuler period. *Proceedings of the 10<sup>th</sup> KACC*, Korea, 1995.
- [8] Britting K. R. *Inertial navigation system analysis*. John Wiley & Sons, 1971.
- [9] Siouris G. M. *Aerospace avionics systems*. Academic press, 1993.